Title

The Raccoon Polyomavirus Genome and Tumor Antigen Transcription Are Stable and Abundant in Neuroglial Tumors

Journal

Journal of Virology, 88(21)

ISSN

0022-538X

Authors

Brostoff, Terza
Dela Cruz, Florante N
Church, Molly E
et al.

Publication Date

2014-11-01

DOI

10.1128/jvi.01912-14

Peer reviewed

JVI Journals.ASM.org

The Raccoon Polyomavirus Genome and Tumor Antigen Transcription Are Stable and Abundant in Neuroglial Tumors

Terza Brostoff, Florante N. Dela Cruz, Jr., Molly E. Church, Kevin D. Woolard, Patricia A. Pesavento

Department of Pathology, Microbiology, and Immunology, School of Veterinary Medicine, University of California, Davis, California, USA

ABSTRACT

Raccoon polyomavirus (RacPyV) is associated with 100% of neuroglial tumors in free-ranging raccoons. Other tumor-associated polyomaviruses (PyVs), including simian virus 40 (SV40), murine PyV, and Merkel cell PyV, are found integrated in the host genome in neoplastic cells, where they constitutively express splice variants of the tumor antigen (TAg) gene. We have previously reported that RacPyV exists only as an episome (nonintegrated) in neuroglial tumors. Here, we have investigated TAg transcription in primary tumor tissue by transcriptome analysis, and we identified the alternatively spliced TAg transcripts for RacPyV. We also determined that TAg was highly transcribed relative to host cellular genes. We further colocalized TAg DNA and mRNA by *in situ* hybridization and found that the majority of tumor cells showed positive staining. Lastly, we examined the stability of the viral genome and TAg transcription by quantitative reverse transcriptase PCR in cultured tumor cells *in vitro* and in a mouse xenograft model. When tumor cells were cultured *in vitro*, TAg transcription increased nearly 2 log-fold over that of parental tumor tissue by passage 17. Both episomal viral genome and TAg transcription were faithfully maintained in culture and in tumors arising from xenotransplantation of cultured cells in mice. This study represents a minimal criterion for RacPyV's association with neuroglial tumors and a novel mechanism of stability for a polyomavirus in cancer.

IMPORTANCE

The natural cycle of polyomaviruses in mammals is to persist in the host without causing disease, but they can cause cancer in humans or in other animals. Because this is an unpredictable and rare event, the oncogenic potential of polyomavirus is primarily evaluated in laboratory animal models. Recently, raccoon polyomavirus (RacPyV) was identified in neuroglial tumors of free-ranging raccoons. Viral copy number was consistently high in these tumors but was low or undetectable in nontumor tissue or in unaffected raccoons. Unlike other oncogenic polyomaviruses, RacPyV was episomal, not integrated, in these tumors. To determine the stability of the viral genome and sustained transcription of the oncogenic tumor antigen genes, we cultured primary raccoon tumor cells and passaged them in mice, confirming the nonintegrated state of the virus and the maintenance of viral gene transcription throughout. RacPyV provides a naturally occurring and tractable model for a novel mechanism of polyomavirus-mediated oncogenesis.

Polyomaviruses (PyVs) infect a wide range of species, including humans. In well-studied PyVs, such as simian virus 40 (SV40), the oncogenic large tumor antigen (LT) protein is necessary and sufficient to transform cells in culture and to create tumors in laboratory animals (1–3). Despite this alarming potential, the typical result of most PyV infections is a détente of long-term, asymptomatic persistence in their host species (4, 5). In 2008, Merkel cell polyomavirus (MCPyV) was discovered as a clonally integrated virus in human Merkel cell carcinoma (MCC), a rare but aggressive skin cancer (6). This is now considered the first example of cancer attributed to naturally occurring PyV infection in humans (7, 8). In 2010, raccoon polyomavirus (RacPyV) was identified in neuroglial olfactory tract tumors of free-ranging raccoons (9). To date, 17 raccoon tumors, all of which harbor abundant viral genome, have been collected from the western United States. RacPyV DNA is comparatively low or undetectable in nontumor brain tissue of affected animals and in unaffected (non-tumor-bearing) animals.

Like other PyVs, RacPyV has a circular double-stranded DNA genome of 5 kb with a noncoding regulatory region (NCRR) dividing the genome into the alternatively spliced early tumor antigen (TAg; nonstructural) region and the late capsid (VP; structural) region (9). RacPyV is closely related to MCPyV at both the genome and protein levels, and they both fall within a monophyletic clade of viruses that some have called almipolyomaviruses, which encode either an overprinting "ALTO" protein or a similarly overprinted middle tumor antigen (MT) protein (10). Almipolyomaviruses include PyVs that are causative for naturally occurring tumors. The RacPyV TAg gene encodes the same predicted immunomodulatory and cellular growth control domains as do other PyVs. However, proof that these gene products contribute to or cause neuroglial tumors in raccoons has so far been limited to epidemiologic data and comparative sequence analyses.

The RacPyV TAg gene encodes predicted large tumor antigen (LT) and small tumor antigen (sT) proteins. Several known oncogenic domains of PyV LT (a DnaJ domain and a retinoblastoma [pRB]-binding motif) and sT (protein phosphatase 2A [PP2A] binding motifs) are present as shown by sequence analysis (9). SV40 LT and sT, along with constitutive overexpression of human

Received 9 July 2014 **Accepted** 19 August 2014

Published ahead of print 27 August 2014

Editor: M. J. Imperiale

Address correspondence to Patricia A. Pesavento, papesavento@ucdavis.edu.

doi:10.1128/JVI.01912-14

telomerase and the H-*ras* oncogene, are sufficient for complete primary cell transformation *in vitro* (11). However, all known PyVs, including those that have never been associated with naturally occurring tumors, encode these predicted oncogenic domains. Therefore, a robust collection of scientific evidence is needed to support the classification of RacPyV as a causative agent in raccoon neuroglial tumors. This is especially critical because RacPyV exists as an episome in raccoon brain tumors, whereas MCPyV is clonally integrated in MCC (9, 12). As a minimal criterion for causality, regardless of its episomal state, we predict that the RacPyV genome and TAg transcription are consistently present in the tumor cell population. Additionally, TAg transcription and its function in tumors should be independent of productive/lytic infection. In the case of MCPyV, this is a result of truncation of LT, either by sequence mutation or by site of integration (7, 13, 14). This occurs at the expense of the structural proteins, which are not required for tumor formation or maintenance and are largely repressed in MCC (15).

In this paper, we demonstrate that episomal RacPyV genome and TAg transcription are abundant in naturally occurring tumors and in a case with metastasis. Furthermore, cultured primary tumor cells inoculated intracranially into immunodeficient Nod-*scid* gamma mice form and recapitulate naturally occurring tumors seen in wild raccoons. In the xenotransplant and in further cell lines cultured from this tissue, episomal RacPyV genome is stable and unaltered and TAg transcript is abundant.

MATERIALS AND METHODS

Transcriptome sequencing. Next-generation sequencing (TruSeq) was utilized for whole-transcriptome analysis of two raccoon brain tumors (Rac 10 and Rac 12) and anatomical location-matched olfactory bulb tissues from two unaffected raccoons. Samples were submitted to the UC Davis Comprehensive Cancer Center's Genomics Shared Resource for RNA isolation, RNA sequencing (RNA-Seq) library preparation and validation, and next-generation sequencing. Rac 10 presented here is the same Rac 10 as that analyzed in the work of Dela Cruz et al., 2013 (9). Detailed procedures are provided below.

RNA isolation. Total cellular RNA was isolated from raccoon brain tumors and normal olfactory bulb tissues (50 mg per sample) using the TRIzol reagent (Life Technologies, Carlsbad, CA) and a modified protocol that incorporates an additional extraction with phenol-chloroform–isoamyl alcohol (25:24:1, pH 4.3). RNA quantity and quality were assessed on a NanoDrop spectrophotometer (Thermo Scientific, Waltham, MA) and an Agilent 2100 Bioanalyzer (Agilent Technologies, Westlake Village, CA), respectively.

Library preparation for RNA-Seq. RNA-Seq libraries were prepared from 1 μg total RNA using the TruSeq RNA sample preparation kit (Illumina, San Diego, CA) according to the manufacturer's protocol. Briefly, polyadenylated mRNA was purified from total RNA and rRNA removed by two rounds of binding to magnetic poly(T) beads. This was followed by RNA fragmentation by incubation in the presence of divalent cations at 94°C for 5 min. Double-stranded cDNA was generated by random-primed first-strand synthesis with SuperScript II reverse transcriptase (Life Technologies) and subsequent second-strand synthesis with RNase H and DNA polymerase I. The cDNA was then blunt ended with T4 and Klenow DNA polymerases to remove 3′ overhangs and fill in 5′ overhangs, phosphorylated with T4 polynucleotide kinase, and then 3′-A tailed by incubation with Klenow fragment (3′→5′ exo–) and dATP. Illumina paired-end adapters were ligated, followed by purification with AMPure XP beads. The library was enriched by high-fidelity PCR amplification (15 cycles) with Phusion DNA polymerase (Thermo Scientific) and adapter-specific primers. The molar concentration of the libraries was determined by measuring concentration with a Qubit fluorometer (Life Technologies), determining the insert length with an Agilent 2100 Bioanalyzer, and then using quantitative PCR (qPCR)-based quantification (KAPA library quantification kit).

Next-generation sequencing and data analysis. Indexed libraries were pooled and loaded on the cBot for cluster generation on TruSeq paired-end flow cells, and paired-end sequencing (2 × 100 bp, paired-end; 4 libraries/lane) was performed with an Illumina HiSeq 2000 sequencing system (BGI@UC Davis Joint Genome Center) using standard Illumina kit reagents (TruSeq SBS kit v3-HS). Image processing, base calling, quality scoring (Phred), FASTQ file generation, and sample demultiplexing were executed by HiSeq control software with real-time analysis (HCS 1.5/RTA 1.13) and CASAVA 1.8 software (Illumina).

Transcriptome analysis. (i) *De novo* transcriptome assembly and analysis. Raw sequencing reads in FASTQ format were subjected to quality trimming and adapter removal with Trimmomatic 0.32 using the following options: ILLUMINACLIP:adapters.fa:2:30:10 TRAILING:3 HEADCROP:15 SLIDINGWINDOW:4:15 MINLEN:70. Quality reads were pooled and used for *de novo* transcriptome assembly using the Trinity platform (r20131110). Assembled transcripts were quantified using RSEM 1.2.7. To reduce the number of artifactually assembled transcripts, transcripts with poor read support (<1 fragment per kilobase of transcript per million fragments mapped [FPKM]) were filtered from the initial assembly. To segregate artifactually assembled false-fusion RacPyV transcripts spanning the NCRR, RacPyV transcripts were separated into early (TAg) and late (VP) regions. The TAg gene was delimited by the start and stop codons of the LT open reading frame (ORF). The structural gene was delimited by the start codon of the VP2 ORF and the stop codon of the VP1 ORF. All retained transcripts were requantified using RSEM and used as the final transcriptome assembly for subsequent analyses. Sequences were annotated via BLASTX (E value, <1e−9) against the UniProtKB/Swiss-Prot database (January 2014 build).

(ii) Read alignment to RacPyV genome. TopHat v2.0.10 and Bowtie 2 v2.1.0 were used to align RNA-Seq reads to the RacPyV genomes and verify splicing events identified in the transcriptome assembly. Quality reads from the two tumor samples were aligned to their respective RacPyV genomes. Quality reads from the two normal olfactory bulb tissues were aligned to RacPyV strain R45 (GenBank accession no. JQ178241.1) (9).

Histology and *in situ* hybridization. Tissues from nine raccoons (Rac 7, Rac 9, Rac 10, Rac 11, Rac 12, Rac 13, Rac 14, Rac 15, and Rac 16) were fixed in 10% buffered formalin, pH 7.2, for at least 48 h and then paraffin embedded. Mouse brains containing xenograft tumors (mouse A1 and mouse A3) were perfused with 4% paraformaldehyde (PFA), followed by overnight fixation and then paraffin embedding. For each tissue, 4-μm sections were processed by standard histologic techniques. Colorimetric *in situ* hybridization (ISH) was performed on Superfrost Plus slides (Fisher Scientific, Pittsburgh, PA) by hand using the RNAscope kit (Advanced Cell Diagnostics, Inc., Hayward, CA) according to the manufacturer's instructions. Briefly, tissue sections were pretreated with heat and protease prior to hybridization with a set of probes complementary to nucleotides (nt) 966 to 2084 of RacPyV R45. A horseradish peroxidase-based signal amplification system was then hybridized to the target probes followed by color development with diaminobenzidine. Slides were counterstained with hematoxylin for 20 s and, following counterstaining, were dipped in xylene and covered with xylene-based SHUR/Mount coverslipping mounting medium (Triangle Biomedical Sciences, Durham, NC), and a coverslip was applied. Positive staining was identified as brown, punctate dots present in the nucleus and/or cytoplasm. Control probes for the bacterial gene DapB (negative control) and for the housekeeping gene ubiquitin C (positive control—evidence of adequate RNA) were included. The raccoon and mouse tissue (and control) slides were read by two veterinary pathologists (P.A.P. and M.E.C.) and classified as either positive or negative. There was no observed hybridization in replicate tissue sections incubated with scrambled (unrelated) probes with similar guanine-cytosine content ($n = 3$), in normal brain tissue within the same section ($n = 6$), or in brain tissues from RacPyV-negative raccoons ($n =$

TABLE 1 Techniques performed with raccoons and mice

Technique or condition	Performance with sample:												
	Rac 7	Rac 9	Rac 10	Rac 11	Rac 12	Rac 13	Rac 14	Rac 14-cultured cells	Rac 15	Rac 16	Mouse A1 and A3	Mouse A2 and A5	Mouse A2- and A5-cultured cells
RNA-Seq			X		X								
In situ hybridization	X	X	X	X	X	X	X		X	X	X		
Southern blot hybridization			X					X					
Xenotransplantation							X						
Sanger sequence	X	X	X	X	X	X	X	X	X	X		X	
Rolling circle amplification			X				X	X				X	
qRT-PCR			X		X			X				X	X
Metastasis present						X							

2). Positive cases had granular cell staining that was above the signal observed on the negative-control slides.

Raccoon cells and primary tumor tissue. Raccoon tumor tissue was collected within 3 h of euthanasia (Rac 14), mechanically homogenized, and cultured as previously described (16). Briefly, tissue was enzymatically dissociated into individual cells and plated into NBE medium consisting of neurobasal medium (Life Technologies), N2 and B27 supplements (0.5× each; Life Technologies), and recombinant human basic fibroblast growth factor (bFGF) and epidermal growth factor (EGF) (25 ng/ml each; R&D Systems, Minneapolis, MN).

Southern blot hybridization and RCA. Southern blot hybridization and rolling circle amplification (RCA) were performed as previously described (9) for Rac 10. Briefly, DNA was extracted using a DNeasy kit according to the manufacturer's instructions (Qiagen, Valencia, CA). For Southern blot hybridization, 1 μg of DNA, undigested or digested with KpnI at 37°C for 16 h, was electrophoresed on a 0.8% agarose gel. Separated DNA was transferred to positively charged nylon membranes (Roche, Indianapolis, IN) overnight by capillary action in 20× SSC (1× SSC is 0.15 M NaCl plus 0.015 M sodium citrate). DNA was UV cross-linked and subsequently hybridized with the RacPyV LT probe previously described (9) at 48°C for 16 h. Membranes were washed with washing buffer (0.1 mol/liter maleic acid, 0.15 mol/liter NaCl; pH 7.5; 0.3% [vol/vol] Tween 20); developed with CDP-Star, ready-to-use (Roche), for up to 15 min; and visualized using a FluorChem E imaging system (ProteinSimple, Santa Clara, CA). RCA was performed on extracted DNA using TempliPhi (GE Healthcare Life Sciences, Piscataway, NJ) according to the manufacturer's instructions for plasmid DNA (1 ng extracted DNA, reaction mixture incubated at 30°C for 14 h).

Mice, xenotransplants, and xenotransplant culture. An intracranial orthotopic xenograft model was used to assess tumorigenicity of cultured cells. Six adult female NSG (NOD.Cg-*Prkdc*^{scid} *Il2rg*^{tm1Wjl}/SzJ) mice were obtained from the UC Davis (UCD) Institute for Regenerative Cures and housed at UCD in accordance with AAALAC regulations. All procedures were reviewed and approved by the UCD Institute for Animal Care and Use Committee. Cells from the raccoon tumor-derived primary cell line (Rac 14) at passage 2 were resuspended in phosphate-buffered saline (PBS), and 5 μl containing 150,000 cells was injected per mouse stereotactically into the striatum (coordinates: 2 mm anterior, 2 mm lateral to bregma, 2.5 mm deep from dura). There was no injection-associated morbidity or mortality. Mice were monitored for weight loss and euthanized at 20% decrease in body weight in accordance with the UCD humane endpoints. Two mice (mouse A2 and mouse A5) were immediately flash-frozen upon euthanasia, and tumors were used for virus DNA sequence verification and homogenized for culture, as described above. Two additional mice (mouse A1 and mouse A3) were perfused, and tissues were immersed in 4% PFA, followed by paraffin embedding, as described above for histology.

PCR and qRT-PCR. DNA from tumors Rac 10 and Rac 12 and from xenotransplant mouse tumors mouse A2 and mouse A5 was extracted using the DNeasy kit as described above (Qiagen). All DNA was amplified by PCR using RacPyV-specific primers, and amplicons were sequenced on an ABI 3730 sequencer (Applied Biosystems, South San Francisco, CA). RCA was performed on both mouse tumors as described above. Total RNA was extracted from Rac 10 and Rac 12; cultured tumor cells from Rac 14 at passage 5 (p5), p10, and p17; and cultured xenotransplant cells from mouse A2 and mouse A5 using the RNeasy kit according to the manufacturer's instructions (Qiagen). RNA was extracted from RacPyV-negative cultured raccoon cortical astrocytes as a negative control. Quantitative reverse transcriptase PCR (qRT-PCR) was performed on an ABI 7300 real-time PCR system (Applied Biosystems) according to the manufacturer's instructions using a probe spanning the exon1/exon2 junction of LT. All samples were assayed in triplicate. The relative quantity of target transcripts was normalized to the number of mammalian 18S rRNA transcripts found in the same samples. The relative quantitation of target gene expression was performed by calculating the comparative cycle threshold (C_T). To verify the mouse brain tumors as true xenotransplants and not primary virus-induced mouse tumors, DNA from two mouse tumors and from the same animals' unaffected brains were extracted as described above and analyzed by PCR using mouse mitochondrial DNA-specific primers.

RESULTS

All raccoons and mice presented in this study are summarized in Table 1.

RacPyV T antigen is highly transcribed in raccoon neuroglial tumors. To investigate RacPyV gene transcription, the tumor tissues of two affected RacPyV-positive raccoons (Rac 10 and Rac 12) were selected for RNA-Seq analysis. Anatomically matched, RacPyV-negative olfactory bulb tissues of two raccoons were included as negative controls. Transcripts were quantified using RNA-Seq by expectation-maximization (RSEM) and annotated using BLASTx homology to the UniProtKB database, and 13,473 protein-coding genes were identified. RacPyV transcripts were detected in both tumor samples, and none were detected in the negative controls.

The two tumor transcriptomes share many common features. With respect to the total polyadenylated RNA population, RacPyV TAg is highly expressed (Fig. 1). In Rac 10 and Rac 12, TAg transcription is estimated to be 61.25 and 532.50 transcripts per million (TPM), respectively. RacPyV structural (VP) gene transcription is reduced relative to that of TAg, estimated at 7.42 and 10.56 TPM in Rac 10 and Rac 12, respectively. Of the 13,473 total genes identified, TAg transcription ranked as the 155th and 2,166th most abundantly transcribed genes and VP ranked 8,784th and 9,339th, respectively.

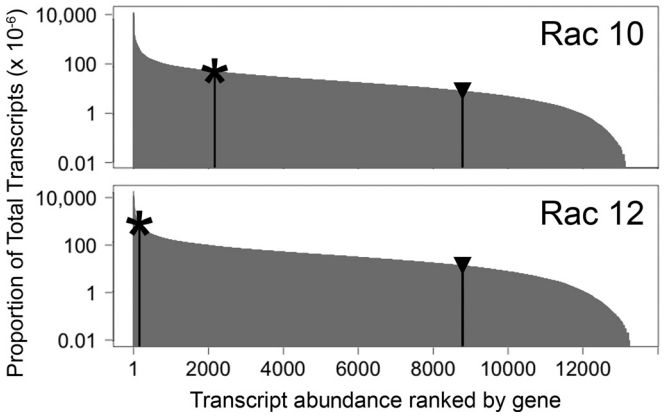

FIG 1 TAg mRNA abundance is high relative to RacPyV VP gene and to total gene transcription in tumors. Total RNA was extracted and filtered for polyadenylated RNA from two RacPyV PCR-positive tumor samples (Rac 10 and Rac 12) and two RacPyV PCR-negative-control olfactory bulbs. RNA was sequenced on an Illumina HiSeq 2000, and pooled quality reads were *de novo* assembled to produce a transcriptome that identified 13,473 protein-coding genes. Transcripts were quantified using RSEM, and genes from the tumor samples were plotted in order of decreasing TPM. Asterisks and inverted triangles indicate RacPyV TAg and VP genes, respectively.

The TAg gene of PyVs encodes a single transcript that is differentially spliced to form numerous proteins necessary for cellular modulation, viral replication, and late gene transcription. While all PyVs encode LT and sT, they also encode a host of other transcripts that are virus specific. In order to determine the range of TAg isoforms generated by tumor-associated RacPyV, we fractionally quantified the TAg transcripts constructed in the *de novo* transcriptome assembly and identified their respective ORFs. Rac 10 and Rac 12 contain different genomic deletions within the LT intron region; consequent transcripts that retain elements of this intron produce unique, tumor-specific TAg ORFs. In general, several isoforms were identified, including LT, sT, MT, and a novel 35kT.

The full-length LT isoform comprises the majority (64% to 66%) of TAg species and encodes the LT-associated motifs classically observed in other polyomaviruses, including the DnaJ domain, the pRB-binding domain, the origin binding domain (OBD), and the helicase domain (Fig. 2). In MCC-associated MCPyV, signature mutations in the viral genome prematurely truncate the LT ORF (7). Similar mutations have not been observed in the genomes of tumor-associated RacPyVs (9). However, a truncated LT ORF may be produced by a subpopulation of mutated RacPyV genomes. To determine if LT ORFs are prema-

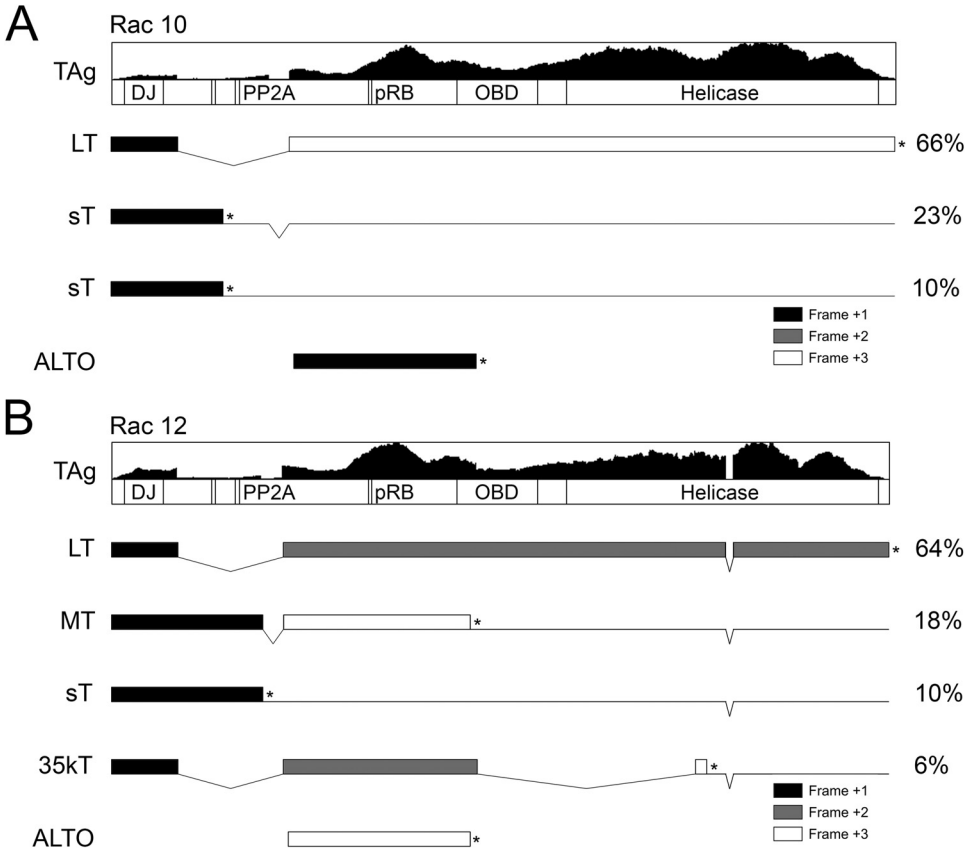

FIG 2 RacPyV TAg isoforms in two tumor samples shown by transcriptome analysis. RacPyV TAg transcripts were detected in two raccoon tumors, Rac 10 (A) and Rac 12 (B). Transcripts were identified by sequence homology to the RacPyV genome R45. Transcripts were quantified by RSEM, and percent abundance of total TAg transcripts was calculated for each isoform (right). Coverage pileups are plotted above a corresponding TAg schematic displaying the associated binding motifs and domains (DJ, DnaJ; PP2A, protein phosphatase 2A binding motif; pRB, retinoblastoma binding domain; OBD, origin binding domain). ORFs are represented by rectangular boxes with stop codons indicated by asterisks, diagonal lines indicate intron splice junctions, and flat lines indicate untranslated regions.

turely truncated, quality reads from tumors were aligned to the constructed LT isoforms and examined for single nucleotide polymorphisms (SNPs) that would prematurely truncate LT. No polymorphisms were detected, suggesting that LT is intact in these tumors. Rac 12 LT contains an intron that splices 7 amino acids out of the helicase domain. This 21-nt intron is estimated to be present in all Rac 12 TAg transcripts but would alter only LT at the level of translation.

The sT isoform is unique in each tumor as a result of differential splicing and genomic composition. In Rac 12, the sequence immediately prior to the sT splice donor site, which is observed in Rac 10, is absent due to the genomic deletion of 522 to 544 bp. Furthermore, no stop codon exists in the Rac 12 LT intron prior to the homologous Rac 10 sT intron sequence, and so a conventional sT ORF does not exist in Rac 12. However, transcripts retaining the LT intron encode an sT ORF defined by a downstream stop codon in the remainder of the LT intron. In Rac 10, the deletion of nucleotide 385 produces a truncated sT ORF that includes only the first of two protein phosphatase 2A (PP2A) binding motifs; the Rac 12 sT ORF includes both of these motifs.

An MT isoform is identified uniquely in Rac 12. The intron observed in Rac 10 sT is also present in Rac 12. However, due to the deletion of 522 to 544 bp in Rac 12, an MT ORF is observed. Similar to the MTs observed in murine PyV, RacPyV MT encodes the DnaJ binding domain, PP2A binding motifs, and the ALTO ORF. No reads spanning the MT intron were observed in Rac 10.

A 35kT isoform is identified uniquely in Rac 12. The 35kT ORF encodes a predicted 35-kDa protein and shares common domains with the similarly designated MCPyV 57kT and SV40 17kT. All three of these proteins contain the DnaJ binding domain and pRB-binding domain. Additionally, their ORFs span three exons by utilizing the LT splice junction and a second downstream splice junction (7, 17). Similarly to MCPyV 57kT, 35kT encodes its exon 2/exon 3 junction within sequences encoding the LT OBD and helicase domains, respectively. Similar to 17kT, the third exon of the 35kT ORF is out of frame with respect to the LT ORF and terminates shortly after the splice junction. No reads spanning the second 35kT intron were observed in Rac 10.

RacPyV TAg gene and transcript localization in neuroglial tumors by *in situ* hybridization. In order to examine spatial, semiquantitative, and cell-specific distribution of RacPyV DNA and mRNA, we performed *in situ* hybridization (ISH) on nine RacPyV tumors using a set of probes complementary to nt 966 to 2084 (exon 2 of LT). The first 320 nt of this region are shared among all predicted splice variants, so this assay can recognize all TAg isoforms. Recognition of transcript alone by ISH is not possible, because RacPyV is a double-stranded DNA virus. Therefore, signal is representative of both viral DNA and mRNA. In one case (Rac 13) where the brain tumor had metastasized to multiple other viscera (lymph node, adrenal gland, and liver), both brain tumor and liver metastases were tested.

TAg ISH was positive in all nine cases, with regionally variable staining in up to 70% of tumor cells (representative subset shown in Fig. 3). No background staining was detectable in any of three different negative-control methods (unrelated size-matched probe, normal brain tissue within the same section, and unaffected raccoons). Colorimetric deposit was primarily detected within the nucleus of the tumor cells; however, signal was often strong, and the deposit frequently exceeded the visual boundary of the nuclear membrane (Fig. 3B, D, F, and H). In areas of tumor where morphology was regionally variable, signal abundance was variable as well (Fig. 3A to F). In areas of necrosis, remnant tumor cells surrounding vascular beds showed particularly strong staining (Fig. 3C and D).

In Rac 13, there was increased abundance of signal in the metastatic cell population of the liver compared to the primary tumor (Fig. 3F and H). Regional staining in the brain tumor on average showed robust staining in 5 to 10% of cells but with approximately 50% of cells showing punctate staining, whereas 100% of the metastatic cells contained robust detectable signal.

A primary cell line cultured from neuroglial tumor retains both episomal viral genome and TAg transcription. We have previously established by two methods (rolling circle amplification [RCA] and Southern blot hybridization) that RacPyV DNA exists as a circular episome in raccoon neuroglial tumors (9). To determine the stability of episomal RacPyV, we generated an *in vitro* culture of tumor cells and examined the maintenance of viral genome and transcription of TAg. Tumor tissue from Rac 10 and cultured cells from Rac 14 were homogenized for Southern blotting. Only episomal, full-length viral DNA was detected (Fig. 4A). The corresponding RCA analysis on both these cells and negative-control cells (cultured RacPyV-negative cortical astrocytes) indicated episomal RacPyV DNA in the tumor tissue and cells only (Fig. 4B).

To verify that tumors and cultured tumor cells were able to transcribe TAg mRNA, quantitative reverse transcriptase PCR (qRT-PCR) was performed on two tumors, Rac 10 and Rac 12, and cultured cells from Rac 14 at p5, p10, and p17. A probe complementary to the LT exon 1/exon 2 splice junction was used. This probe excluded detection of sT and MT transcripts but included all other TAg isoforms. Cultured RacPyV-negative cortical astrocytes were used as a negative control. Using 18S rRNA as a control for cellular input, TAg was highly transcribed in Rac 10 and Rac 12, demonstrating 25- and 15-fold increases over cortical astrocytes, respectively (Fig. 5). TAg transcription increased over time in cultured cells from Rac 14, from approximately a 1,200-fold increase over baseline tumor transcription at p5 to approximately a 3,000-fold increase by p17.

Xenotransplants in immunodeficient mice and a subsequent primary cell line stably maintain RacPyV TAg and recapitulate original tumor. We next tested whether this tumor could be reproduced *in vivo*, and, if so, if this selective environment would affect the stability of RacPyV genome or TAg transcription. We injected a minimally expanded primary cell culture (p2) from Rac 14 orthotopically into six immunodeficient (Nod-*scid* gamma) mice. Tumors formed in all six mice, with a median survival time of 61 days (Fig. 6). Based on mitochondrial DNA amplification and sequencing, tumor tissue was of raccoon origin and not a result of *de novo* viral infection and transformation (data not shown). Two xenograft tumors (mouse A2 and mouse A5) tested positive for RacPyV genome by PCR and/or RCA. Virus was sequenced and matched the parental tumor with perfect sequence identity (data not shown).

Sublocalization and abundance of viral genome and TAg transcripts were assessed by ISH in 2 mice (mouse A1 and mouse A3) and compared to the Rac 14 parental tumor. ISH in xenotransplants recapitulated the distribution and quantity of signal seen in the raccoon tumor tissue (Fig. 7). Like Rac 14, morphology was regionally variable in the mice and TAg expression was similarly variable, with staining in up to 70% of cells (Fig. 7B and D).

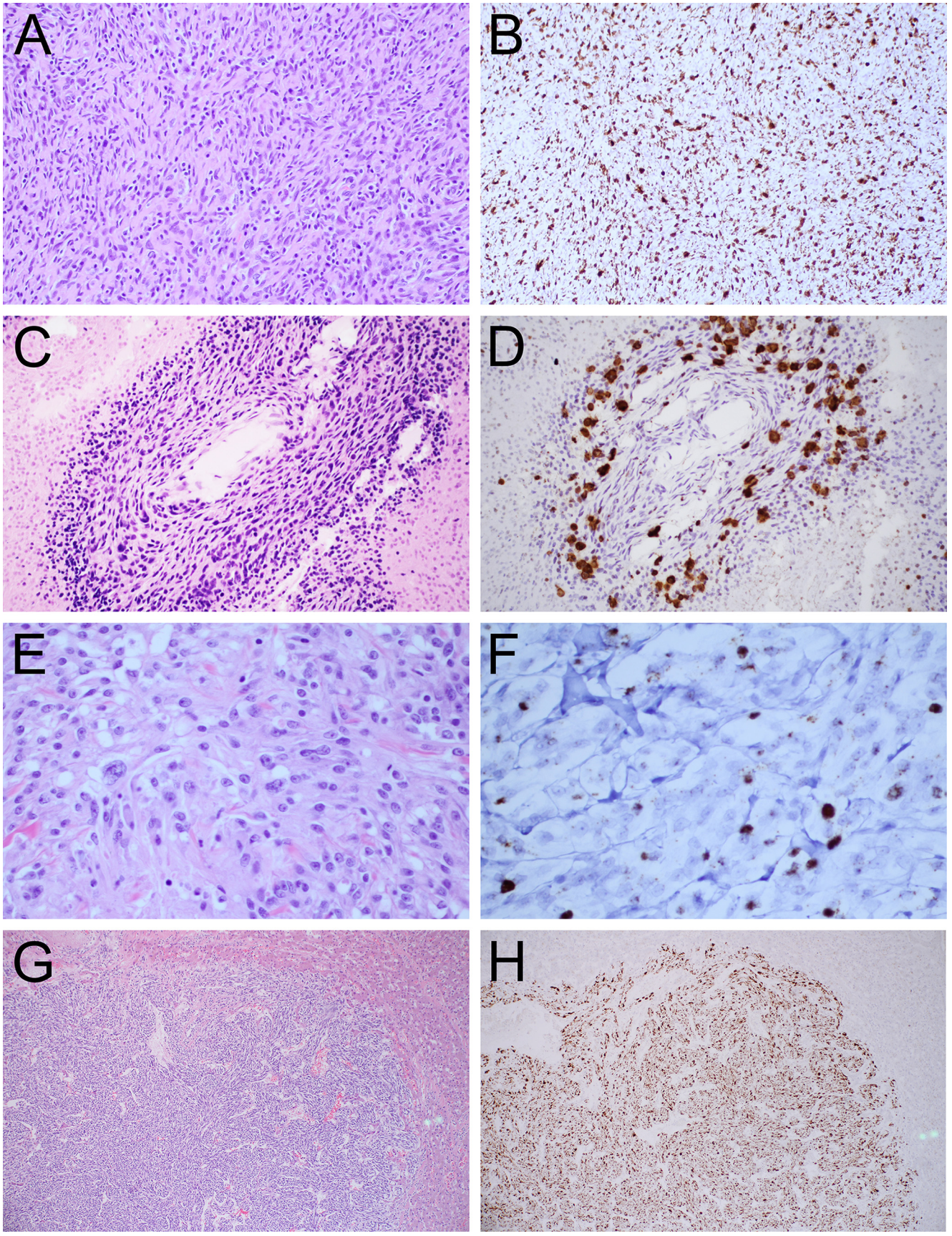

FIG 3 Histology and detection of RacPyV genome and TAg mRNA by *in situ* hybridization. Raccoon tumors were formalin fixed and paraffin embedded prior to staining. (A and B) Hematoxylin and eosin staining (A) and ISH (B) from Rac 15, a representative neuroglial tumor. (C and D) Hematoxylin and eosin staining (C) and ISH (D) from Rac 9 with increased signal around an area of necrosis. (E to H) Hematoxylin and eosin staining (E) and ISH (F) from the parental tumor of Rac 13, with liver metastases (G and H) showing less variability and greater staining than the parental tumor.

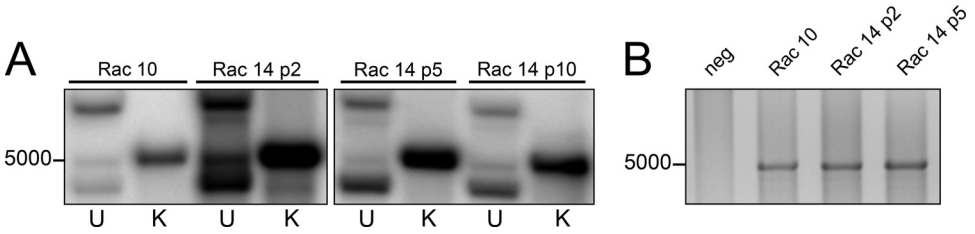

FIG 4 Episomal RacPyV genome is maintained in cell culture by Southern blotting and RCA. (A) Southern blot hybridization against RacPyV of Rac 10 tumor tissue and Rac 14 tumor-derived cell culture at passages 2, 5, and 10. (B) RCA of Rac 10 tumor tissue and Rac 14 tumor-derived cell culture at passages 2 and 5. U, undigested; K, KpnI digested; neg, negative control (raccoon cortical astrocytes).

To verify and quantify TAg gene expression, qRT-PCR was performed on cells cultured from mouse A2 and mouse A5 using the probe for RacPyV TAg as described above. As seen with cells cultured from primary raccoon tumor, low-passage-number (p2) cells from each xenotransplant demonstrated an increase above parental tumor, showing ~300- and ~100-fold increases, respectively (data not shown).

DISCUSSION

RacPyV is associated with all neuroglial tumors found to date in free-ranging raccoons and has the potential to provide a natural model for PyV-mediated tumorigenesis. These tumors maintain the virus genome and express high levels of TAg mRNA even when subjected to selective or foreign environments, including passage in culture and growth in immunocompromised mice. Overall, this study provides evidence for RacPyV TAg as a necessary driver of raccoon neuroglial tumors.

While the positions of introns are similar in RacPyV TAg compared to other PyVs, the resulting ORFs are different, both between RacPyV tumors and between RacPyV and other PyVs. The differences seen in RacPyV TAg introns compared to other PyVs could explain differences in viral replication or transcription in neuroglial tumors. However, because these differences in sequence (including SNPs and deletions) are not consistent among viral isolates, they are unlikely to be important for the formation or maintenance of tumors. Limitations of transcriptome analysis include the detection of preprocessed mRNA, which could explain some of the differences in introns seen in this study. Additionally, short reads cannot be assigned to their parent transcripts when those reads are ambiguously mapped (multiple reads which could map to one of several transcripts). However, we can calculate percent abundance of transcripts by using the RNA-Seq expectation-maximization, a statistical model that proportionally allocates ambiguous reads based on unambiguous (uniquely mapped) reads (18). Despite our ability to calculate percent abundance of transcripts, mRNA is a proxy for protein expression and isoforms seen by transcript analysis are not necessarily translated in abundance. Further work is needed to detect protein isoforms present in these tumors.

In both Rac 10 and Rac 12, TAg is highly transcribed relative to VP, and LT is the dominant isoform of TAg transcribed. The disproportionately high level of TAg transcription relative to VP transcription occurs without an apparent truncation in LT by either a mutation or an integration event. Among potential mechanisms for this control are those used by other viruses, including sequence rearrangements in the NCRR in disease-associated compared to shed virus, histone deacetylase- or DNA methyltransferase-mediated gene silencing, and virus- or host cell-encoded microRNA-mediated silencing (19, 20). The ALTO transcript cannot be verified because its ORF is contained within all other TAg transcripts. Furthermore, we cannot currently determine whether or not the protein is expressed.

In other known carcinogenic viruses, including MCPyV and papillomaviruses, integration is considered an early and critical step in transformation (6, 21). In these cases, integration serves at

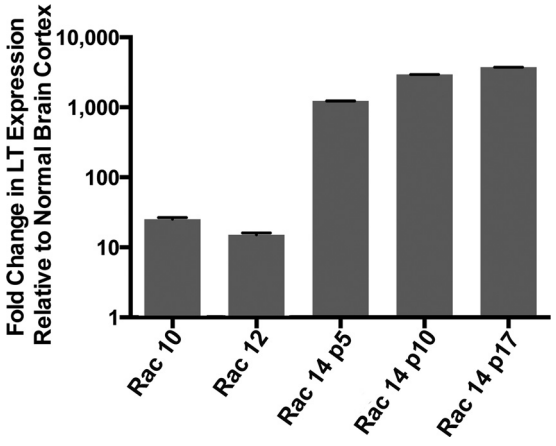

FIG 5 TAg mRNA is expressed in tumors and increases over time in cultured primary tumor cells by qRT-PCR. Raccoon tumor tissue from Rac 10 and Rac 12 and cultured cells from Rac 14 at passages 5, 10, and 17 were assayed for RacPyV TAg by qRT-PCR, normalized for 18S rRNA. Fold change is relative to RacPyV-negative cortical astrocytes.

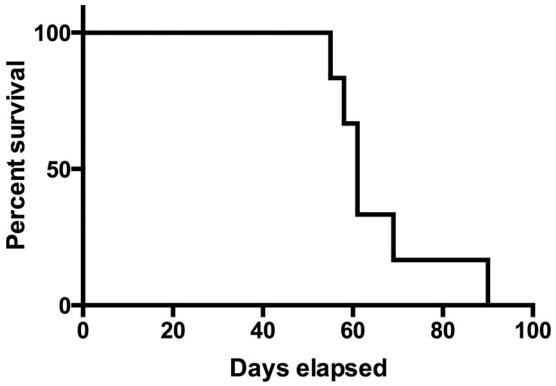

FIG 6 Raccoon xenograft survival curve. Six Nod-*scid* gamma mice were injected with 150,000 p2 tumor cells from Rac 14. Percent survival is plotted against days postinjection.

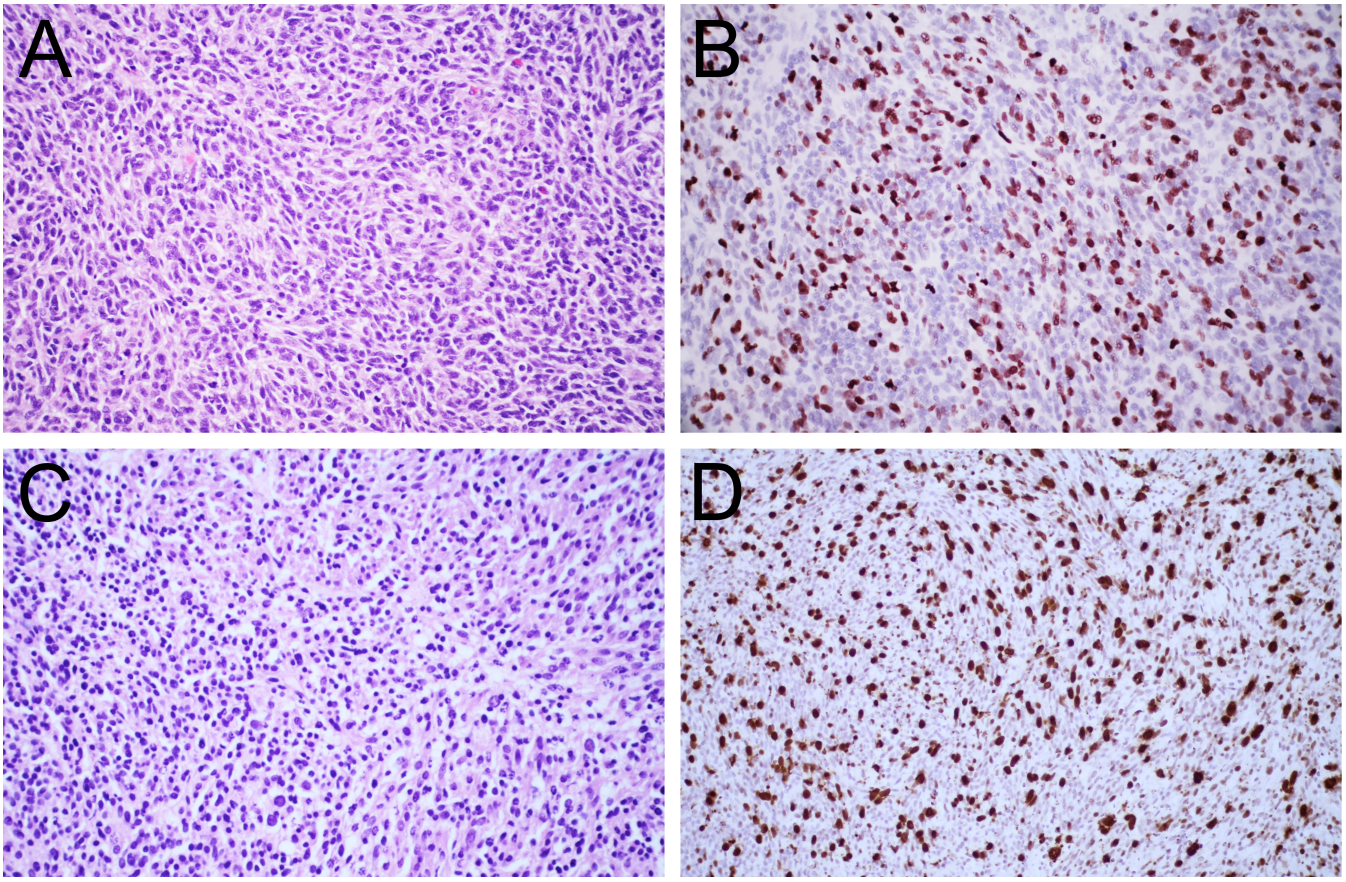

FIG 7 Histologic phenotype and ISH of RacPyV genome and TAg mRNA of parental raccoon tumor and xenotransplant tumor in mice. Parental tumor from Rac 14 (A and B) was cultured and used for xenotransplant in mice. Tumors were formalin fixed and paraffin embedded prior to staining. Representative Mouse A3 (C and D) highlighting similarity by hematoxylin and eosin staining (A and C) and ISH (B and D) to parental Rac 14.

least two purposes: to stabilize the virus genome so that it is faithfully segregated in replicated cells and to inhibit productive/lytic infection via decreased expression of structural proteins in the cell, favoring instead early gene expression (14, 22, 23). Here, we have shown that both maintenance of viral genome and selective TAg (and not VP) transcription occur in tumors in the absence of integration. Many other viruses are able to maintain genome segregation without integration in dividing populations of cells. Potential alternative mechanisms by which RacPyV achieves this are abundant. Among these, the virus could use physical genome stabilization within these tumors, such as chromatin tethering, as seen in papillomavirus or herpesvirus infection (12, 24). Alternatively, regardless of physical genome stabilization, virus could be selected for by the cells carrying it, to the exclusion of cells dividing at a lower rate (cells which either have not replicated viral genome or have insufficient TAg expression).

In addition to analyses that demonstrate the presence of RacPyV genome and TAg transcription, we performed ISH, which allows direct visualization of TAg mRNA and DNA in tissue. The tumor cells had regionally variable staining, with most of the cells strongly positive. In the single raccoon in which tumor cells had metastasized to other organs, staining was consistent and robust in all of the metastatic cells within the liver. Unfortunately, metastatic tissue available was fixed and embedded and was of insufficient quality to perform Southern blotting or RCA analysis to determine if viral genome had integrated in this singular case.

Our data are highly suggestive of the requirement for RacPyV and specifically TAg in the development and maintenance of neuroglial tumors. Identification of TAg protein isoforms present in tumors and protein-protein interactions between TAg and host cellular proteins will prove useful in evaluating novel mechanisms of polyomavirus stability in tumors and will contribute to a scientific understanding of virus-associated transformation. In representing the only nonhuman spontaneous PyV-associated oncogenic transformation, the RacPyV/neuroglial tumor relationship could serve as a natural model of recognized and potentially novel mechanisms of PyV-associated oncogenesis.

ACKNOWLEDGMENTS

We thank Ryan R. Davis and Stephenie Y. Liu (GSR and Department of Pathology and Laboratory Medicine) for their expert technical support for the next-generation sequencing studies.

The UC Davis Comprehensive Cancer Center Genomics Shared Resource is supported by Cancer Center support grant P30 CA093373 (R.W. dV.W.) from the NCI. This study was funded by Bernice Barbour Foundation grant 11-58N.

REFERENCES

1. **Manfredi JJ, Prives C.** 1994. The transforming activity of simian virus 40 large tumor antigen. Biochim. Biophys. Acta **1198:**65–83.

2. **Van Dyke TA, Finlay C, Miller D, Marks J, Lozano G, Levine AJ.** 1987. Relationship between simian virus 40 large tumor antigen expression and tumor formation in transgenic mice. J. Virol. **61:**2029–2032.
3. **Pipas JM.** 2009. SV40: cell transformation and tumorigenesis. Virology **384:**294–303. http://dx.doi.org/10.1016/j.virol.2008.11.024.
4. **Kean JM, Rao S, Wang M, Garcea RL.** 2009. Seroepidemiology of human polyomaviruses. PLoS Pathog. **5:**e1000363. http://dx.doi.org/10.1371/journal.ppat.1000363.
5. **DeCaprio JA, Garcea RL.** 2013. A cornucopia of human polyomaviruses. Nat. Rev. Microbiol. **11:**264–276. http://dx.doi.org/10.1038/nrmicro2992.
6. **Feng H, Shuda M, Chang Y, Moore PS.** 2008. Clonal integration of a polyomavirus in human Merkel cell carcinoma. Science **319:**1096–1100. http://dx.doi.org/10.1126/science.1152586.
7. **Shuda M, Feng H, Kwun HJ, Rosen ST, Gjoerup O, Moore PS, Chang Y.** 2008. T antigen mutations are a human tumor-specific signature for Merkel cell polyomavirus. Proc. Natl. Acad. Sci. U. S. A. **105:**16272–16277. http://dx.doi.org/10.1073/pnas.0806526105.
8. **Arora R, Chang Y, Moore PS.** 2012. MCV and Merkel cell carcinoma: a molecular success story. Curr. Opin. Virol. **2:**489–498. http://dx.doi.org/10.1016/j.coviro.2012.05.007.
9. **Dela Cruz FN, Jr, Giannitti F, Li L, Woods LW, Del Valle L, Delwart E, Pesavento PA.** 2013. Novel polyomavirus associated with brain tumors in free-ranging raccoons, western United States. Emerg. Infect. Dis. **19:**77–84. http://dx.doi.org/10.3201/eid1901.121078.
10. **Carter JJ, Daugherty MD, Qi X, Bheda-Malge A, Wipf GC, Robinson K, Roman A, Malik HS, Galloway DA.** 2013. Identification of an overprinting gene in Merkel cell polyomavirus provides evolutionary insight into the birth of viral genes. Proc. Natl. Acad. Sci. U. S. A. **110:**12744–12749. http://dx.doi.org/10.1073/pnas.1303526110.
11. **Hahn WC, Dessain SK, Brooks MW, King JE, Elenbaas B, Sabatini DM, DeCaprio JA, Weinberg RA.** 2002. Enumeration of the simian virus 40 early region elements necessary for human cell transformation. Mol. Cell. Biol. **22:**2111–2123. http://dx.doi.org/10.1128/MCB.22.7.2111-2123.2002.
12. **Bastien N, McBride AA.** 2000. Interaction of the papillomavirus E2 protein with mitotic chromosomes. Virology **270:**124–134. http://dx.doi.org/10.1006/viro.2000.0265.
13. **Houben R, Shuda M, Weinkam R, Schrama D, Feng H, Chang Y, Moore PS, Becker JC.** 2010. Merkel cell polyomavirus-infected Merkel cell carcinoma cells require expression of viral T antigens. J. Virol. **84:**7064–7072. http://dx.doi.org/10.1128/JVI.02400-09.
14. **Cheng J, Rozenblatt-Rosen O, Paulson KG, Nghiem P, Decaprio JA.** 2013. Merkel cell polyomavirus large T antigen has growth-promoting and inhibitory activities. J. Virol. **87:**6118–6126. http://dx.doi.org/10.1128/JVI.00385-13.
15. **Pastrana DV, Tolstov YL, Becker JC, Moore PS, Chang Y, Buck CB.** 2009. Quantitation of human seroresponsiveness to Merkel cell polyomavirus. PLoS Pathog. **5:**e1000578. http://dx.doi.org/10.1371/journal.ppat.1000578.
16. **Son MJ, Woolard K, Nam DH, Lee J, Fine HA.** 2009. SSEA-1 is an enrichment marker for tumor-initiating cells in human glioblastoma. Cell Stem Cell **4:**440–452. http://dx.doi.org/10.1016/j.stem.2009.03.003.
17. **Ibelgaufts H, Doerfler W, Scheidtmann KH, Wechsler W.** 1980. Adenovirus type 12-induced rat tumor cells of neuroepithelial origin: persistence and expression of the viral genome. J. Virol. **33:**423–437.
18. **Li B, Dewey CN.** 2011. RSEM: accurate transcript quantification from RNA-Seq data with or without a reference genome. BMC Bioinformatics **12:**323. http://dx.doi.org/10.1186/1471-2105-12-323.
19. **Gosert R, Kardas P, Major EO, Hirsch HH.** 2010. Rearranged JC virus noncoding control regions found in progressive multifocal leukoencephalopathy patient samples increase virus early gene expression and replication rate. J. Virol. **84:**10448–10456. http://dx.doi.org/10.1128/JVI.00614-10.
20. **White MK, Safak M, Khalili K.** 2009. Regulation of gene expression in primate polyomaviruses. J. Virol. **83:**10846–10856. http://dx.doi.org/10.1128/JVI.00542-09.
21. **Schwarz E, Freese UK, Gissmann L, Mayer W, Roggenbuck B, Stremlau A, zur Hausen H.** 1985. Structure and transcription of human papillomavirus sequences in cervical carcinoma cells. Nature **314:**111–114. http://dx.doi.org/10.1038/314111a0.
22. **Laude HC, Jonchere B, Maubec E, Carlotti A, Marinho E, Couturaud B, Peter M, Sastre-Garau X, Avril MF, Dupin N, Rozenberg F.** 2010. Distinct Merkel cell polyomavirus molecular features in tumour and non tumour specimens from patients with Merkel cell carcinoma. PLoS Pathog. **6:**e1001076. http://dx.doi.org/10.1371/journal.ppat.1001076.
23. **Stoler MH, Rhodes CR, Whitbeck A, Wolinsky SM, Chow LT, Broker TR.** 1992. Human papillomavirus type 16 and 18 gene expression in cervical neoplasias. Hum. Pathol. **23:**117–128. http://dx.doi.org/10.1016/0046-8177(92)90232-R.
24. **Ilves I, Kivi S, Ustav M.** 1999. Long-term episomal maintenance of bovine papillomavirus type 1 plasmids is determined by attachment to host chromosomes, which Is mediated by the viral E2 protein and its binding sites. J. Virol. **73:**4404–4412.